Performance analysis of a residential photovoltaic string under partial shading

Byunggyu Yu[1], Youngseok Jung[2]
[1]Division of Electrical, Electronic and Control Engineering, Regional-Industrial Application Research Institute and Institute of IT Convergence Technology, Kongju National University, Cheonan-si, Republic of Korea
[2]Photovoltaics Research Department, Korea Institute of Energy Research, Daejeon-si, Republic of Korea

Article Info

Article history:

Received Apr 18, 2022
Revised Jul 28, 2022
Accepted Aug 15, 2022

Keywords:

Number of MPPs
Partial shading
Photovoltaic generation
Power loss
Photovoltaic modules
Photovoltaic residential
Photovoltaic string

ABSTRACT

As one of the most prominent renewable energy resources, Photovoltaic (PV) generation has been growing dramatically over the last years and its applications are classified into residential, commercial, and power plant class, based on its power capacity. Especially, a typical residential PV system has been configured with serially connected PV modules. For serially connected PV modules, shading is a critical factor to reduce the whole string PV output power. This paper presents study on performance analysis of a residential PV string under partial shading. This analysis contains how many maximum power points (MPPs) occur and how much power would be lost while a PV string is under partial shading with different shading positions and different shading intensities. PSIM simulation tool is used to verify the performance analysis. As a result, the number of MPPs is directly related with the number of shading intensities, regardless of the shading position. In this paper, it was verified that 8 maximum power points were generated for 8 solar intensities regardless of the location of the shadows under extreme conditions. These results can be utilized for fault diagnosis in the PV string.

Corresponding Author:

Byunggyu Yu
Division of Electrical, Electronic and Control Engineering and Institute of IT Convergence Technology
Kongju National University, 1223-24 Cheonan Daero
Seobuk-gu, Cheonan-Si, Chungnam, 330-717, Republic of Korea
Email: suttichai@mail.com

1. INTRODUCTION

Renewable energy is energy that has been derived from earth's natural resources that are not finite or exhaustible, such as wind and sunlight. Renewable energy is an alternative to the traditional energy that relies on fossil fuels, and it tends to be much less harmful to the environment [1]–[3]. Photovoltaic (PV) generation is one of the most popular power generation sources among renewable energy sources, and worldwide growth of PV is extremely dynamic [4], [5]. By the end of 2019, a cumulative amount of 629 GW of solar power was installed throughout the world [6]. PV generates electric power by using PV modules to convert energy from the sunlight into a flow of electrons by the photovoltaic effect [7].

PV markets are classified into three segments: residential [8], [9], commercial [10], [11], and PV power plant [12]–[14]. Especially, residential PV application ranges. Most residential PV typically feature a capacity of about less than 10 kW, while commercial PV often reaches to 100 kW and PV power plant over 100 kW [15]. Especially, PV modules for typical 3 kW residential PV application in Korea are connected in series to match with PV inverter input voltage specification with single string [16]–[18]. For serially connected PV string, shading is a critical factor to reduce the whole string PV output power [19]–[23]. Up to now, the partial shading problems are analyzed partly based on a few string conditions [24]–[26].

This paper presents study on performance analysis of a residential PV string under partial shading. The relation between number of MPPs and the amount of reduced power in PV string configuration by the shading effect is to be dealt with in general. In order words, this analysis contains how many MPPs occur and how much power would be lost while a PV string is under partial shading with different shading positions and different shading intensities.

In this paper, typical specification of a PV string system is introduced first for various case studies. Then, analysis of both power loss analysis and number of MPPs are presented under partial shading. Finally, PSIM simulation results are provided in order to verify the performance.

2. THE PROPOSED SYSTEM DESIGN

In this study, an analysis is performed when a shadow occurs in a single PV string system, which is a typical residential PV system configuration. In order to model a typical 3 kW class PV residential system as shown in Figure 1(a), a 360 W commercial PV module specification is selected for a component of PV string. In addition, it is assumed that eight PV modules are connected in series to make a typical residential PV string power as 2,880 W as shown in Figures 1(b) and 1(c). Quantitative specification for PV module and PV string are presented in Table 1. The study is based on comprehensive shading effects by shading positions and shading intensities as shown in Tables 2 and 3.

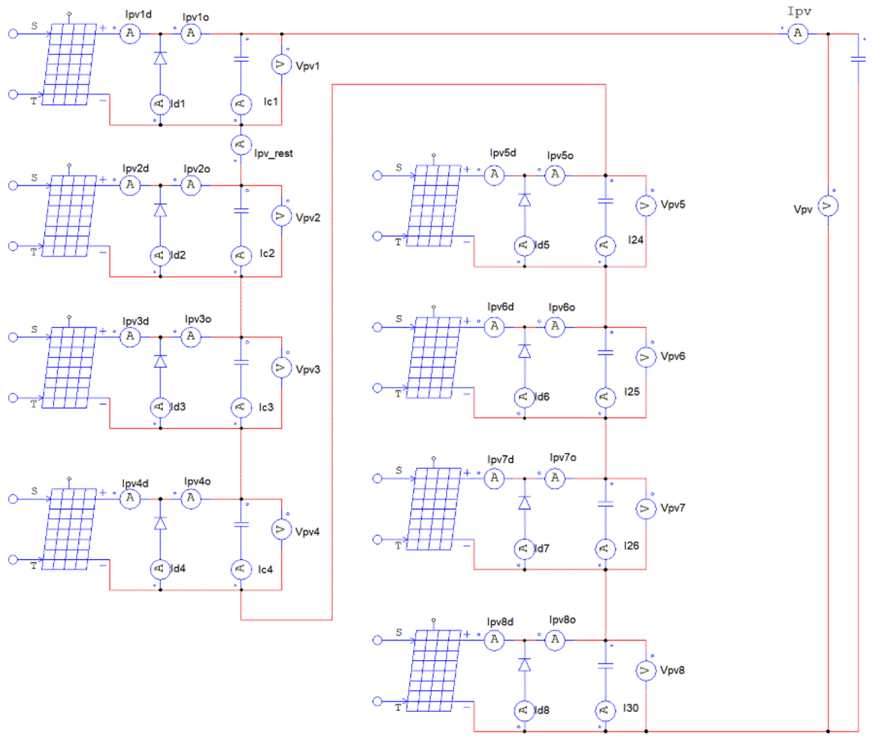

(a)

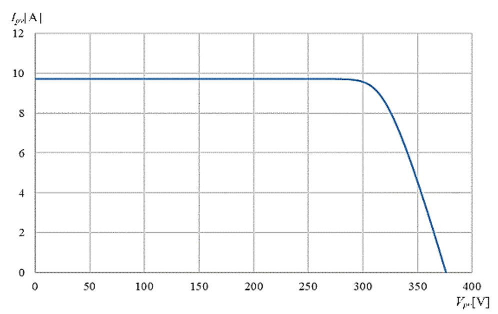

(b)

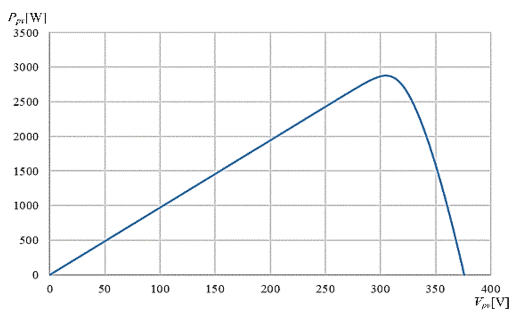

(c)

Figure 1. A typical PV string configuration (a) simulation circuit model, (b) voltage-power characteristics curve at standard test condition, and (c) voltage-power characteristics curve at standard test condition

Table 1. A typical electric specification for residential PV string configuration

Parameter	Value	
	PV module	PV string
Open circuit voltage, V_{oc}	47 [V]	376 [V]
Short circuit current, I_{sc}	9.72 [A]	9.72 [A]
Voltage at maximum power at STC, V_{mp}	38 [V]	304 [V]
Current at maximum power at STC, I_{mp}	9.47[A]	9.47 [A]
Maximum power, P_{max}	360 [W]	2880 [W]
Number of series connected PV modules	-	8
Temperature, T	25 °C	25 °C

STC: standard test condition

Firstly, after setting the shading intensity to 500 W/m^2, the effect was compared and analyzed while changing the location of the shadow, as shown in Table 2. From A1 to A8, the shadow position was changed while the number of shadows was fixed at one. From A9 to A15, when a shadow occurred on two modules, the shadow was fixed on PV module #1, and the position of the remaining shadow module was changed from PV module #2 to #8. From A16 to A21, the shadow was fixed on both PV #1 and #2, and the remaining one was changed from PV #3 to PV #8. From A22 to A26, the shadow was placed on both PV #1 and #3, and the other one was changed from PV #4 to #8. Under the above conditions, according to the location where the shadow of the same intensity occurs in the PV string connected in series, the number of PV maximum power points (MPPs) and the generation loss are analyzed. Lastly, in order to analyze the effect of different shadow intensities generated from the residential solar string, the shadow intensity for cases B1 to B7 was set to have a difference of 100 W/m^2 from 900 to 300 W/m^2. Then, the effect of when the shadows were sequentially generated from PV #1 to module #7 was comparatively analyzed.

Table 2. Shading positioning configuration

<table>
<tr><th>Case No.</th><th>No. of shading</th><th>No. of shading intensity</th><th colspan="8">Shading intensity [W/m²]</th></tr>
<tr><th></th><th></th><th></th><th>PV#1</th><th>PV#2</th><th>PV#3</th><th>PV#4</th><th>PV#5</th><th>PV#6</th><th>PV#7</th><th>PV#8</th></tr>
<tr><td>A1</td><td>1</td><td>1</td><td>500</td><td colspan="7">1,000</td></tr>
<tr><td>A2</td><td>1</td><td>1</td><td>1,000</td><td>500</td><td colspan="6">1,000</td></tr>
<tr><td>A3</td><td>1</td><td>1</td><td colspan="2">1,000</td><td>500</td><td colspan="5">1,000</td></tr>
<tr><td>A4</td><td>1</td><td>1</td><td colspan="3">1,000</td><td>500</td><td colspan="4">1,000</td></tr>
<tr><td>A5</td><td>1</td><td>1</td><td colspan="4">1,000</td><td>500</td><td colspan="3">1,000</td></tr>
<tr><td>A6</td><td>1</td><td>1</td><td colspan="5">1,000</td><td>500</td><td colspan="2">1,000</td></tr>
<tr><td>A7</td><td>1</td><td>1</td><td colspan="6">1,000</td><td>500</td><td>1,000</td></tr>
<tr><td>A8</td><td>1</td><td>1</td><td colspan="7">1,000</td><td>500</td></tr>
<tr><td>A9</td><td>2</td><td>1</td><td colspan="2">500</td><td colspan="6">1,000</td></tr>
<tr><td>A10</td><td>2</td><td>1</td><td>500</td><td>1,000</td><td>500</td><td colspan="5">1,000</td></tr>
<tr><td>A11</td><td>2</td><td>1</td><td>500</td><td colspan="2">1,000</td><td>500</td><td colspan="4">1,000</td></tr>
<tr><td>A12</td><td>2</td><td>1</td><td>500</td><td colspan="3">1,000</td><td>500</td><td colspan="3">1,000</td></tr>
<tr><td>A13</td><td>2</td><td>1</td><td>500</td><td colspan="4">1,000</td><td>500</td><td colspan="2">1,000</td></tr>
<tr><td>A14</td><td>2</td><td>1</td><td>500</td><td colspan="5">1,000</td><td>500</td><td>1,00</td></tr>
<tr><td>A15</td><td>2</td><td>1</td><td>500</td><td colspan="6">1,000</td><td>500</td></tr>
<tr><td>A16</td><td>3</td><td>1</td><td colspan="3">500</td><td colspan="5">1,000</td></tr>
<tr><td>A17</td><td>3</td><td>1</td><td colspan="2">500</td><td>1,000</td><td>500</td><td colspan="4">1,000</td></tr>
<tr><td>A18</td><td>3</td><td>1</td><td colspan="2">500</td><td colspan="2">1,000</td><td>500</td><td colspan="3">1,000</td></tr>
<tr><td>A19</td><td>3</td><td>1</td><td colspan="2">500</td><td colspan="3">1,000</td><td>500</td><td colspan="2">1,000</td></tr>
<tr><td>A20</td><td>3</td><td>1</td><td colspan="2">500</td><td colspan="4">1,000</td><td>500</td><td>1,000</td></tr>
<tr><td>A21</td><td>3</td><td>1</td><td colspan="2">500</td><td colspan="5">1,000</td><td>500</td></tr>
<tr><td>A22</td><td>3</td><td>1</td><td>500</td><td>1,000</td><td colspan="2">500</td><td colspan="4">1,000</td></tr>
<tr><td>A23</td><td>3</td><td>1</td><td>500</td><td>1,000</td><td>500</td><td>1,000</td><td>500</td><td colspan="3">1,000</td></tr>
<tr><td>A24</td><td>3</td><td>1</td><td>500</td><td>1,000</td><td>500</td><td colspan="2">1,000</td><td>500</td><td colspan="2">1,000</td></tr>
<tr><td>A25</td><td>3</td><td>1</td><td>500</td><td>1,000</td><td>500</td><td colspan="3">1,000</td><td>500</td><td>1,000</td></tr>
<tr><td>A26</td><td>3</td><td>1</td><td>500</td><td>1,000</td><td>500</td><td colspan="4">1,000</td><td>500</td></tr>
</table>

Table 3. Shading intensity configuration

<table>
<tr><th>Case No.</th><th>No. of shading</th><th>No. of shading intensity</th><th>Shading strength [W/m²]</th><th colspan="8">Shading intensity [W/m²]</th></tr>
<tr><th></th><th></th><th></th><th></th><th>PV#1</th><th>PV#2</th><th>PV#3</th><th>PV#4</th><th>PV#5</th><th>PV#6</th><th>PV#7</th><th>PV#8</th></tr>
<tr><td>B1</td><td>2</td><td>2</td><td>1000</td><td>900</td><td>800</td><td colspan="6">1000</td></tr>
<tr><td>B2</td><td>3</td><td>3</td><td>1000</td><td>900</td><td>800</td><td>700</td><td colspan="5">1000</td></tr>
<tr><td>B3</td><td>4</td><td>4</td><td>1000</td><td>900</td><td>800</td><td>700</td><td>600</td><td colspan="4">1000</td></tr>
<tr><td>B4</td><td>5</td><td>5</td><td>1000</td><td>900</td><td>800</td><td>700</td><td>600</td><td>500</td><td colspan="3">1000</td></tr>
<tr><td>B5</td><td>6</td><td>6</td><td>1000</td><td>900</td><td>800</td><td>700</td><td>600</td><td>500</td><td>400</td><td colspan="2">1000</td></tr>
<tr><td>B6</td><td>7</td><td>7</td><td>1000</td><td>900</td><td>800</td><td>700</td><td>600</td><td>500</td><td>400</td><td>300</td><td>1000</td></tr>
</table>

3. RESULTS AND DISCUSSION

In this section, we analyze the power generation loss and the number of maximum power points by analyzing the voltage-current and voltage-power characteristic curves according to the location and intensity of the shadow in the solar string. If solar irradiance, temperature, power generation amount, solar output voltage and output current. Are measured in the field, it is possible to diagnose failures such as shadows in residential PV string and defective solar modules based on the data presented in this paper.

3.1. Shading position effects

Figures 2(a) to 2(d) shows the voltage-current characteristic curve when the shadow of the same intensity changes depending on the position in the PV string, under case A1 to A26. Figure 3 shows the voltage-power characteristic curve under the same conditions. Table 4 shows power loss analysis results by different shading positions for a PV string, including number of MPP, main information of local maximum power point (LMPP). The efficiency in Table 4 is defined as the ratio of output in LMPP to output in standard test condition (STC) 1,000 W/m^2 and 25 $°C$.

In cases A1 to A8 as shown in Figure 2(a), the shadow occurs in one module at 500 W/m^2, but the location of the shadow is different for each module. One of the modules has a shadow intensity of 500 W/m^2 and the rest is 1,000 W/m^2, indicating that the type of short-circuit current is divided into two. In Figure 2(b), two shadows occur with two kinds of intensity, and Figures 2(c) and 2(d) show that three shadows occur with two kinds of intensity. It can be seen that the same two short-circuit current type occurs.

Figure 3 shows voltage-power characteristic curves for PV string under different shading positions. As shown in Figure 3(a), two different LMPPs are identified, and the larger value is called as global maximum power point (GMPP). From A1 to A8, GMPP is formed as 2,519 W at PV voltage 267 V. If the solar intensity is two types, it can be confirmed that the MPP is also two with the same PV voltage/current/power characteristic curves. In cases A9 to A15 as shown in Figure 3(b), shadows are generated on two modules at 500 W/m^2, but the location of occurrence is different. Although the number of shaded PV modules increases compared to cases A1 to A8, the number of MPPs is also two because there are still two types of solar intensity. From A9 to A15, GMPP is formed as 2,159 W at PV voltage 229 V. In the same way, For the cases A16 to A26 as shown in Figures 3(c) and 3(d), the number of shaded PV modules increases to three, but the type of shadow intensity is constant as one 500 W/m^2, so it can be seen that they have the same solar light characteristic curve and power generation characteristic, as shown in Figures 2 and 3. However, since the shadow intensity is applied differently for each module, it is important to look at the effect of shadows occurring in the PV string. This point will be explored in the next section.

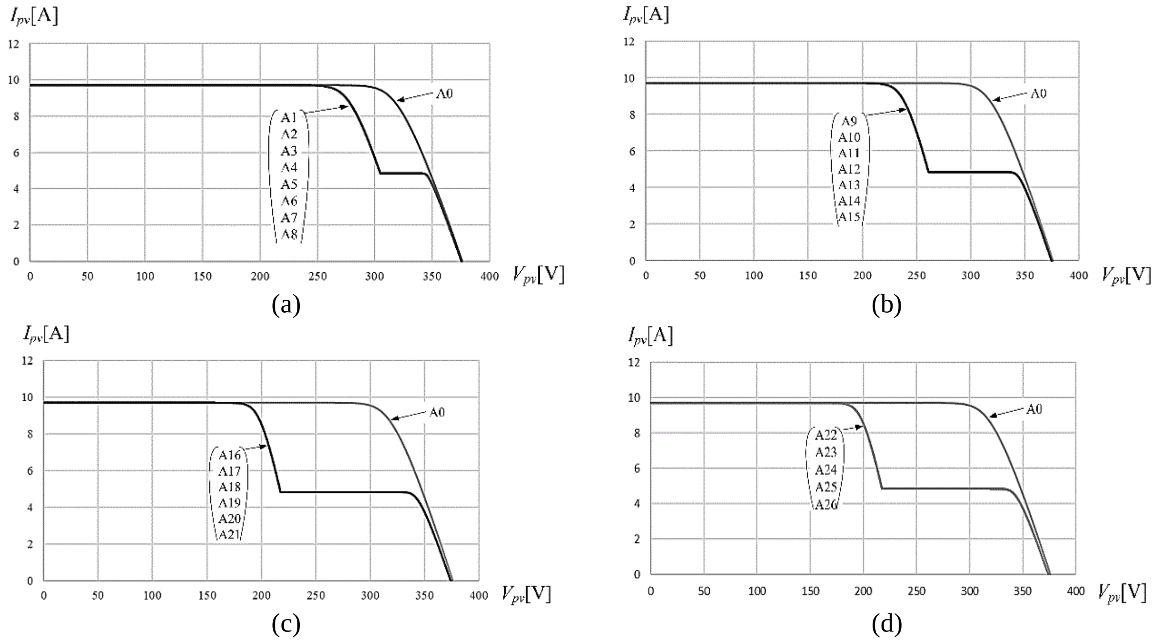

Figure 2. Voltage-current characteristic curves for PV string under different shading positions: (a) from case A1 to case A8, (b) from case A9 to case A15, (c) from case A16 to case A21, and (d) from case A22 to case A26

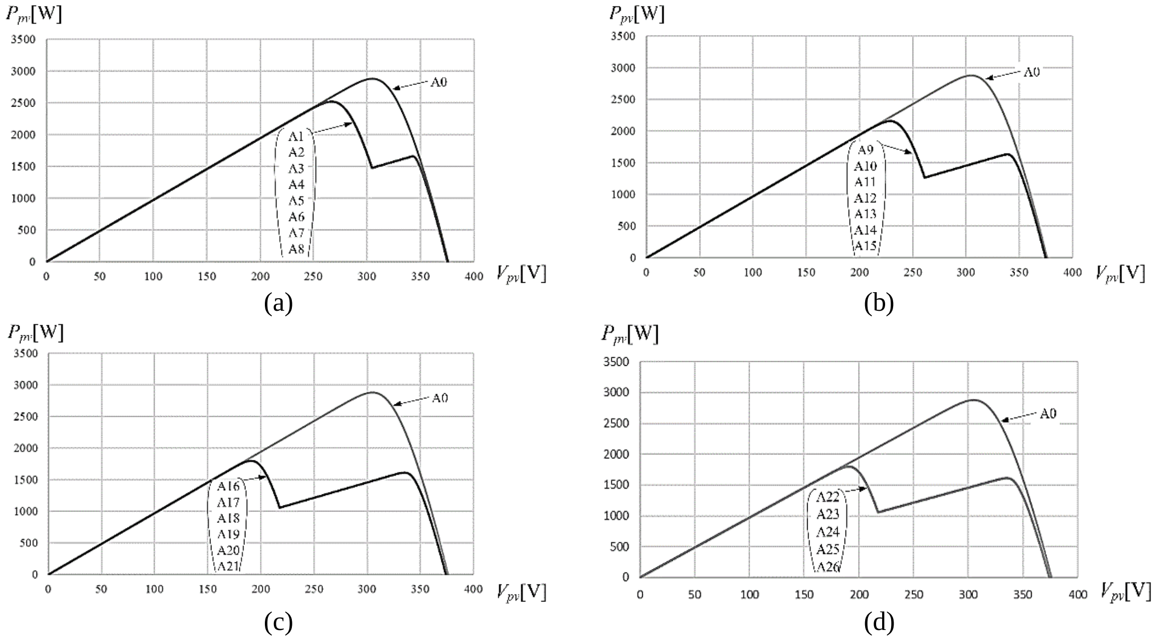

Figure 3. Voltage-power characteristic curves for PV string under different shading positions: (a) from case A1 to case A8, (b) from case A9 to case A15, (c) from case A16 to case A21, and (d) from case A22 to case A26

Table 4. Power loss analysis results by different shading positions for a PV string

Case No.	Shading intensity [W/m^2]	No. of MPP	LMPP1 (GMPP)			LMPP2		
			V_{pv}	P_{pv}	Eff.	V_{pv}	P_{pv}	Eff.
A1	500	2	267	**2519**	87%	343	1656	58%
A2								
A3								
A4								
A5								
A6								
A7								
A8								
A9	500	2	229	**2159**	75%	339	1633	57%
A10								
A11								
A12								
A13								
A14								
A15								
A16	500	2	191	**1799**	62%	335	1612	56%
A17								
A18								
A19								
A20								
A21								
A22	500	2	191	**1799**	62%	335	1612	56%
A23								
A24								
A25								
A26								

3.2. Shading intensity effects

Multiple maximum power points are generated in the solar module through the bypass of the solar module in the condition where the shadow effect occurs. Analyzing the effect with a formula is as follows:
If the shaded solar intensity is *Irr_1, Irr_2, ..., Irr_n* in descending order of magnitude,

$$V_{pv,max,Irr\_1} \times \mathrm{N} = V_{pv,max1} \quad (3)$$

$$V_{pv,max,Irr\_2} \times (\mathrm{N} - 1) = V_{pv,max2} \quad (4)$$

$$V_{pv,max,Irr\_n} \times (\mathrm{N} - \mathrm{n}) = V_{pv,maxn} \quad (5)$$

$$V_{pv,max1} \times I_{pv,max,Irr\_1} = P_{pv,max1} \quad (6)$$

$$V_{pv,max2} \times I_{pv,max,Irr\_2} = P_{pv,max2} \quad (7)$$

$$V_{pv,maxn} \times I_{pv,max,Irr\_n} = P_{pv,maxn} \quad (8)$$

where $V_{pv,max,\ Irr\_n}$ is the voltage at the maximum power of a single PV module with shading intensity *Irr_n*, *N* is the number of series connected PV modules for PV string, $V_{pv,maxn}$ is the voltage at the local maximum power of a PV string with shading intensity *Irr_n*, and I_{pv,max,Irr_n} is the current at the local maximum power of a PV string with shading intensity *Irr_n*. $P_{pv,max1}$, $P_{pv,max2}$, *and* $P_{pv,maxn}P$ are the local maximum power point respectively under different shading intensities.

Figure 4(a) to (f) shows the voltage-current characteristic curve when the intensity of the shadow in the solar string varies according to the position, Figure 5(a) to (f) shows the voltage-power characteristic curve. Table 5 shows the LMPPs and the tracking efficiency compared to the STC condition. In case B1, three types of solar intensity according to shadow are formed, and as shown in Figure 4(a), the resulting short-circuit current is divided into three types. Accordingly, as shown in Figure 5(a), three maximum power points were formed by three types of short-circuit current types. As shown in (6), the maximum power point voltage/current of the unit module in the solar radiation condition of 800 W/m^2 is connected in 8 series to form an LMPP. In the solar condition of 900 W/m^2, the maximum power point voltage/current of the unit module is connected in 7 series to form LMPP, and Finally, the maximum power point voltage/current of the unit module in the solar radiation condition of 1,000 W/m^2 is 6 in series to form the LMPP. Among them, GMPP is formed with the largest value, and according to Table 5, among them, GMPP is 2,498 W, and the voltage at that time is 323 V.

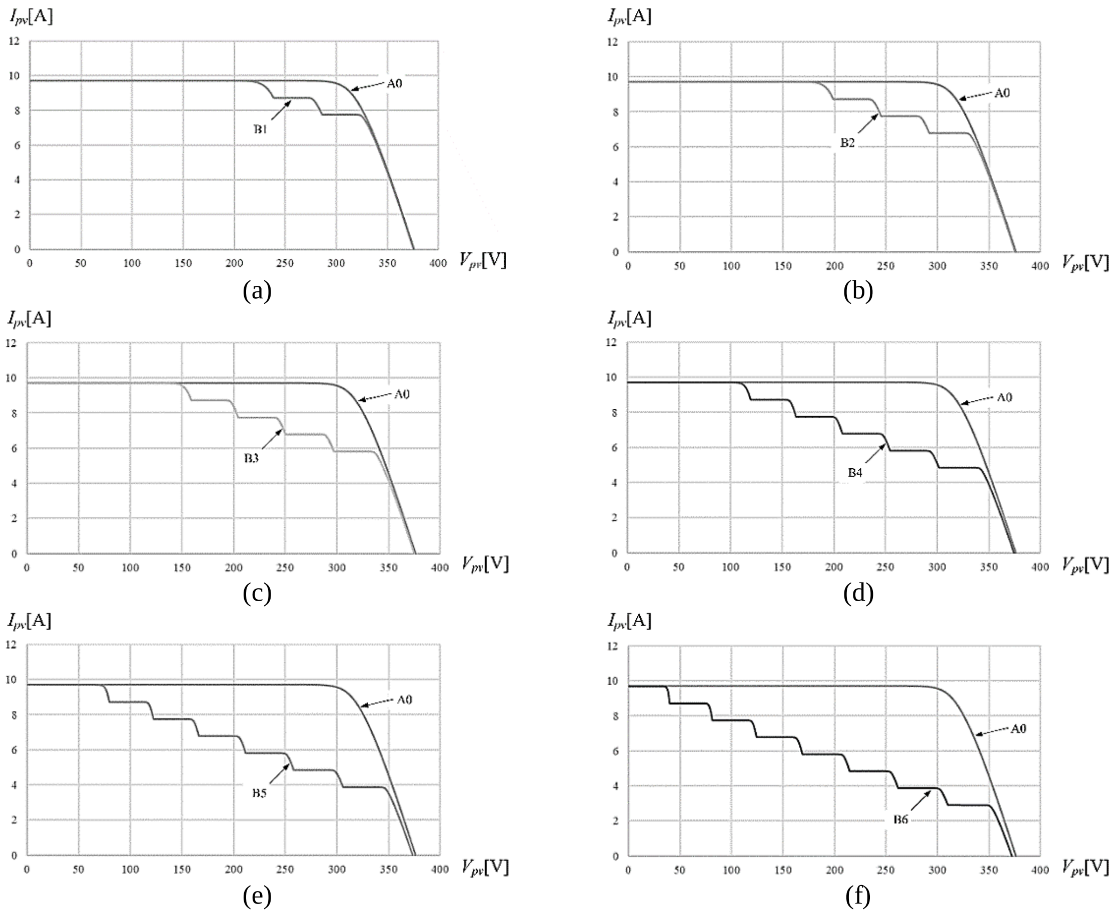

Figure 4. Voltage-current characteristic curves for PV string under different shading intensities. (a) B1, (b) B2, (c) B3, (d) B4, (e) B5, and (f) B6

Table 5. Power loss analysis results by different shading intensities for a PV string

Case No.	No. of MPP	Shading intensity [W/m^2]	LMPP1			LMPP2			LMPP3			LMPP4			LMPP5			LMPP6			LMPP7			LMPP8		
			V_{pv}	P_{pv}	Eff.	V_{pv}	P_{pv}	Eff.	V_{pv}	P_{pv}	Eff.	V_{pv}	P_{pv}	Eff.	V_{pv}	P_{pv}	Eff.	V_{pv}	P_{pv}	Eff.	V_{pv}	P_{pv}	Eff.	V_{pv}	P_{pv}	Eff.
B1	3	1000 900 800	323	**2498**	87%	276	2394	83%	229	2159	75%															
B2	4	1000 900 800 700	330	**2228**	77%	283	2182	76%	236	2049	71%	191	1799	62%												
B3	5	1000 900 800 700 600	335	1941	67%	288	**1945**	68%	242	1865	65%	197	1703	59%	152	1439	50%									
B4	6	1000 900 800 700 600 500	340	1641	57%	292	**1693**	59%	246	1661	58%	201	1549	54%	177	1370	48%	114	1079	37%						
B5	7	1000 900 800 700 600 500 400	344	1331	46%	296	1431	50%	250	**1445**	50%	204	1378	48%	160	1233	43%	117	1013	35%	76	719	25%			
B6	8	1000 900 800 700 600 500 400 300	349	1011	35%	300	1160	40%	253	**1221**	42%	207	1198	42%	163	1095	38%	119	917	32%	78	669	23%	38	359	12%

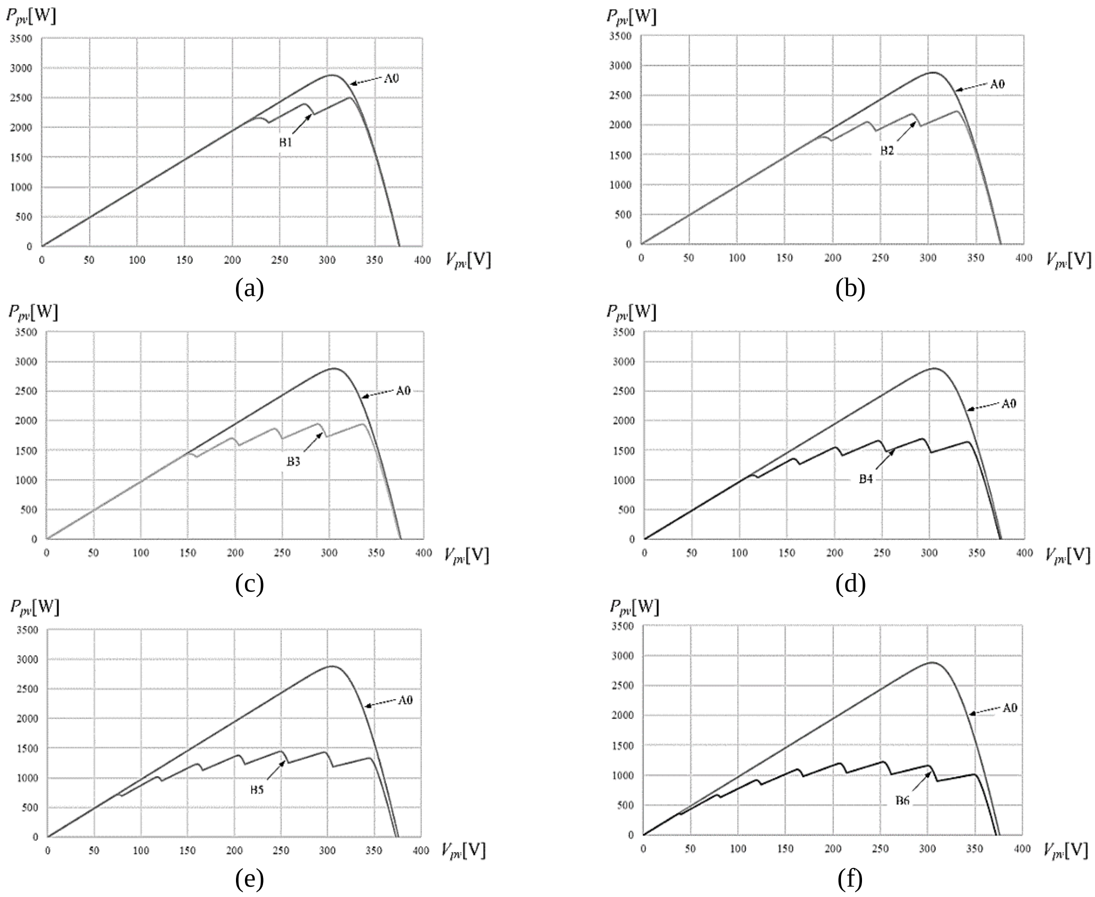

Figure 5. Voltage-power characteristic curves for PV string under different shading intensities: (a) B1, (b) B2, (c) B3, (d) B4, (e) B5, and (f) B6

In the same way, Figures 4(b) to 4(f) shows voltage-current characteristic curves for PV string under different shading intensities from cased B2 and B7, respectively. The number of maximum power points is determined according to the number of types of solar intensities from cases B2 to B7, as shown in Figures 5(b) to 5(f), respectively. GMPP is determined as the largest value among them in Table 5. Through the above analysis, it can be confirmed that the number of LMPPs is determined according to the number of types of solar intensity, and the largest value among them does not always exist at a constant position, and the position is determined as the largest value among LMPPs.

4. CONCLUSION

In this paper, a performance analysis on the effect of shadows in a residential solar system is presented. If the shadowed PV modules were generated with the same shadow intensity, it was confirmed that the number of LMPPs was the same regardless of the location of the shadow, and the related characteristic curves were also the same.

When the intensity of the shadow generated by each module of the solar string is different, the number of LMPPs was determined by the number of types of shadow intensity, and the largest value GMPP among them was not always presented at a certain shaded position. In this paper, it was verified that eight maximum power points were generated for eight solar intensities regardless of the location of the shadows under extreme conditions. Using the results of this paper as basic data, it is expected to be able to diagnose the cause of failures in PV string such as shadow effects or module defects.

ACKNOWLEDGEMENTS

This work was supported by the research grant of the Kongju National University in 2021" and "This work was supported by the National Research Foundation of Korea (NRF) grant funded by the Korea government (MSIT) (No. 2021R1F1A1050199)".

REFERENCES

[1] W. C. Sinke, "Development of photovoltaic technologies for global impact," *Renewable Energy*, vol. 138, pp. 911–914, Aug. 2019, doi: 10.1016/j.renene.2019.02.030.

[2] R. Li and F. Shi, "Control and optimization of residential photovoltaic power generation system with high efficiency isolated bidirectional DC–DC converter," *IEEE Access*, vol. 7, pp. 116107–116122, 2019, doi: 10.1109/ACCESS.2019.2935344.

[3] B. Yu and S.-C. Ko, "Power dissipation analysis of PV module under partial shading," *International Journal of Electrical and Computer Engineering (IJECE)*, vol. 11, no. 2, pp. 1029–1035, Apr. 2021, doi: 10.11591/ijece.v11i2.pp1029-1035.

[4] S. Eftekharnejad, G. T. Heydt, and V. Vittal, "Optimal generation dispatch with high penetration of photovoltaic generation," *IEEE Transactions on Sustainable Energy*, vol. 6, no. 3, pp. 1013–1020, Jul. 2015, doi: 10.1109/TSTE.2014.2327122.

[5] P. A. J. Stecanella, D. Vieira, M. V. L. Vasconcelos, and A. D. L. Ferreira Filho, "Statistical analysis of photovoltaic distributed generation penetration impacts on a utility containing hundreds of Feeders," *IEEE Access*, vol. 8, pp. 175009–175019, 2020, doi: 10.1109/ACCESS.2020.3024115.

[6] T. Tang, H. Ding, S. Nojavan, and K. Jermsittiparsert, "Environmental and economic operation of wind-PV-CCHP-based energy system considering risk analysis Via downside risk constraints technique," *IEEE Access*, vol. 8, pp. 124661–124674, 2020, doi: 10.1109/ACCESS.2020.3006159.

[7] Y. Mahmoud and E. El-Saadany, "Accuracy improvement of the ideal PV model," *IEEE Transactions on Sustainable Energy*, vol. 6, no. 3, pp. 909–911, Jul. 2015, doi: 10.1109/TSTE.2015.2412694.

[8] Y. Sun, S. Li, B. Lin, X. Fu, M. Ramezani, and I. Jaithwa, "Artificial neural network for control and grid integration of residential solar photovoltaic systems," *IEEE Transactions on Sustainable Energy*, vol. 8, no. 4, pp. 1484–1495, Oct. 2017, doi: 10.1109/TSTE.2017.2691669.

[9] M. T. A. Khan, G. Norris, R. Chattopadhyay, I. Husain, and S. Bhattacharya, "Autoinspection and permitting with a PV utility interface (PUI) for residential plug-and-play solar photovoltaic unit," *IEEE Transactions on Industry Applications*, vol. 53, no. 2, pp. 1337–1346, Mar. 2017, doi: 10.1109/TIA.2016.2631135.

[10] S. Martín, J. Pérez-Ruiz, and P. López-Pérez, "Model to evaluate the system-wide impact of residential and commercial photovoltaic and storage units intended for self-consumption," *IET Renewable Power Generation*, vol. 13, no. 12, pp. 2111–2122, Sep. 2019, doi: 10.1049/iet-rpg.2019.0228.

[11] N. K. Kandasamy, K. Kandasamy, and K. J. Tseng, "Loss-of-life investigation of EV batteries used as smart energy storage for commercial building-based solar photovoltaic systems," *IET Electrical Systems in Transportation*, vol. 7, no. 3, pp. 223–229, Sep. 2017, doi: 10.1049/iet-est.2016.0056.

[12] X. Li, W. Li, Q. Yang, W. Yan, and A. Y. Zomaya, "An unmanned inspection system for multiple defects detection in photovoltaic plants," *IEEE Journal of Photovoltaics*, vol. 10, no. 2, pp. 568–576, Mar. 2020, doi: 10.1109/JPHOTOV.2019.2955183.

[13] A. M. M. Sizkouhi, M. Aghaei, S. M. Esmailifar, M. R. Mohammadi, and F. Grimaccia, "Automatic boundary extraction of large-scale photovoltaic plants using a fully convolutional network on aerial imagery," *IEEE Journal of Photovoltaics*, vol. 10, no. 4, pp. 1061–1067, Jul. 2020, doi: 10.1109/JPHOTOV.2020.2992339.

[14] T. Kohno *et al.*, "Fault-diagnosis architecture for large-scale photovoltaic power plants that does not require additional sensors," *IEEE Journal of Photovoltaics*, vol. 9, no. 3, pp. 780–789, May 2019, doi: 10.1109/JPHOTOV.2019.2903870.

[15] D. Chung, C. Davidson, R. Fu, K. Ardani, and R. Margolis, "U.S. photovoltaic prices and cost breakdowns: Q1 2015 benchmarks for residential, commercial, and utility-scale system," National Renewable Energy Laboratory, 2015.

[16] D. W. H. Cai, S. Adlakha, S. H. Low, P. De Martini, and K. M. Chandy, "Impact of residential PV adoption on retail electricity rates," *Energy Policy*, vol. 62, pp. 830–843, Nov. 2013, doi: 10.1016/j.enpol.2013.07.009.
[17] Y. Li, W. Gao, and Y. Ruan, "Performance investigation of grid-connected residential PV-battery system focusing on enhancing self-consumption and peak shaving in Kyushu, Japan," *Renewable Energy*, vol. 127, pp. 514–523, Nov. 2018, doi: 10.1016/j.renene.2018.04.074.
[18] M. Boztepe, F. Guinjoan, G. Velasco-Quesada, S. Silvestre, A. Chouder, and E. Karatepe, "Global MPPT scheme for photovoltaic string inverters based on restricted voltage window search algorithm," *IEEE Transactions on Industrial Electronics*, vol. 61, no. 7, pp. 3302–3312, Jul. 2014, doi: 10.1109/TIE.2013.2281163.
[19] A. S. Rana, M. Nasir, and H. A. Khan, "String level optimisation on grid-tied solar PV systems to reduce partial shading loss," *IET Renewable Power Generation*, vol. 12, no. 2, pp. 143–148, Feb. 2018, doi: 10.1049/iet-rpg.2017.0229.
[20] M. A. Mohamed, A. A. Z. Diab, and H. Rezk, "Partial shading mitigation of PV systems via different meta-heuristic techniques," *Renewable Energy*, vol. 130, pp. 1159–1175, Jan. 2019, doi: 10.1016/j.renene.2018.08.077.
[21] O. Bingöl and B. Özkaya, "Analysis and comparison of different PV array configurations under partial shading conditions," *Solar Energy*, vol. 160, pp. 336–343, Jan. 2018, doi: 10.1016/j.solener.2017.12.004.
[22] J. Ma, X. Pan, K. L. Man, X. Li, H. Wen, and T. On Ting, "Detection and assessment of partial shading scenarios on photovoltaic strings," *IEEE Transactions on Industry Applications*, vol. 54, no. 6, pp. 6279–6289, Nov. 2018, doi: 10.1109/TIA.2018.2848643.
[23] P. Bharadwaj and V. John, "Optimized global maximum power point tracking of photovoltaic systems based on rectangular power comparison," *IEEE Access*, vol. 9, pp. 53602–53616, 2021, doi: 10.1109/ACCESS.2021.3071136.
[24] K. A. Kim and P. T. Krein, "Reexamination of photovoltaic hot spotting to show inadequacy of the bypass diode," *IEEE Journal of Photovoltaics*, vol. 5, no. 5, pp. 1435–1441, Sep. 2015, doi: 10.1109/JPHOTOV.2015.2444091.
[25] S. Mishra, H. Ziar, O. Isabella, and M. Zeman, "Selection map for PV module installation based on shading tolerability and temperature coefficient," *IEEE Journal of Photovoltaics*, vol. 9, no. 3, pp. 872–880, May 2019, doi: 10.1109/JPHOTOV.2019.2900695.
[26] M. Dhimish, "70% decrease of hot-spotted photovoltaic modules output power loss using novel MPPT algorithm," *IEEE Transactions on Circuits and Systems II: Express Briefs*, vol. 66, no. 12, pp. 2027–2031, Dec. 2019, doi: 10.1109/TCSII.2019.2893533.

BIOGRAPHIES OF AUTHORS

Byunggyu Yu was born in Korea, in 1976. He received the BS and MS degrees in electrical engineering from Pusan University, Korea, in 2000 and from KAIST in 2002, respectively. Since 2002, he had been with the Korea Institute of Energy Research as a Research Fellow. In 2007, he started his RONPAKU doctoral degree program supported by a scholarship from the government of Japan at the Tokyo Polytechnic University, and he received the PhD degree in electrical engineering in 2010. Since 2012, he has been with Kongju National University as an assistant professor. His research interests include photovoltaic system including the module-integrated converter system and its control algorithm. He can be contacted at email: bgyuyu@kongju.ac.kr.

Youngseok Jung was born in Korea, in 1970. He received the BS and MS degrees in electrical engineering from Chungbuk National University, South Korea, in 1994 and in 1996, respectively. Since 1996, he had been with the Korea Institute of Energy Research as a Research Fellow. In 2002, he started his doctoral degree program at Chungbuk National University, and he received the PhD degree in electrical engineering in 2006. His research interests include photovoltaic system and its control algorithm. He can be contacted at email: jung96@kier.re.kr.